Ultrasonic Nondestructive Evaluation Techniques Applied to the Quantitative Characterization of Textile Composite Materials

I. Introduction

In this Progress Report, we describe our development of advanced ultrasonic nondestructive evaluation methods applied to the characterization of anisotropic materials. We discuss the use of an ultrasonic wave propagation model in conjunction with measured data to enhance the understanding of the physics underlying the interaction of ultrasound with anisotropic materials, such as multiaxial warp-knit composites and other fiber-reinforced specimens. We present images obtained from experimental measurements and simulations of ultrasonic fields in water. Furthermore, the simulation is extended to produce images of ultrasonic field propagation through a woven fiber composite material with values of the anisotropy of the attenuation coefficient based on knowledge of previous work by our group.[1] For reasons of image resolution, all images have been included on the accompanying CD-ROM both in JPEG format and in Adobe™ Portable Document Format (PDF).

In Section II of this Progress Report we describe the implementation of the ultrasonic wave propagation model we employed. In addition, we briefly address concerns related to the ultrasonic beam, such as diffraction and phase cancellation across the face of a finite-aperture, phase-sensitive receiving transducer. Section III describes the experimental arrangement and methods for acquiring the ultrasonic diffraction patterns. Following the description of the data acquisition technique, Section IV details the analysis of the experimental data and the methods of the simulations. In Section V, the resulting images of the ultrasonic diffraction patterns derived from experimental data are compared with model simulations (See CD-ROM for images). A discussion of the observations and conclusions are found in Section VI.

II. Background

The overall goal of this research is to enhance the understanding of the scientific principles necessary to successfully develop advanced ultrasonic materials characterization methods required for the inspection of complex fiber-reinforced material structures. A specific goal of our proposed research is to understand the fundamental physics underlying the interaction of ultrasonic fields with the inherent physical properties of these complex material structures. This includes developing an understanding of how ultrasonic fields propagate in these materials by examining the propagation of the phase-fronts and energy of the ultrasound in these inherently anisotropic materials.

In order to develop a robust measurement method for nondestructive evaluation of anisotropic materials, it is necessary to have an understanding of the diffraction of the ultrasonic field within the media. Diffraction of the ultrasonic field can occur for a variety of reasons, including the intrinsic nature of a specific sample (specific intrinsic textile composite parameters, i.e., tow sizes, layup configuration, etc.), surface roughness (both random and periodic), external stitching, and inhomogeneities. In addition, the experimental sampling of the ultrasonic field may be compromised due to phase cancellation effects across the face of the receiving transducer[2,3]. Computer simulations can be utilized in developing a more fundamental understanding of the effects that phase-distorting anisotropic materials can have on the diffraction pattern and propagation characteristics of the interrogating ultrasonic wave.

There are a number of ultrasonic wave propagation models available for numerical implementation, such as the Measurement Model[4], the Wisconsin Method[5,6] and the Angular Spectral Decomposition method[7-12], to name a few. Each model has its advantages. The Angular Spectral Decomposition method offers a numerically efficient algorithm. For this reason, as a first step we have chosen to employ the Angular Spectral Decomposition method as a tool for modeling our experimental arrangements.

Approach

Our approach toward understanding the diffraction of ultrasound within anisotropic materials is to progress systematically from structurally simple specimens to more complex structured composite specimens. This systematic approach facilitates the understanding of how increasing structural complexity affects the ultrasonic diffraction pattern. Initial investigations of ultrasonic diffraction patterns were conducted in water only. Subsequent investigations modeled the effects of inserting a woven fiber composite specimen into the ultrasonic field.

III. Experimental Arrangement / Method

All measurements in this study were performed in an immersion tank using a 0.5" diameter, spherically-focused (2" focal length), piezoelectric transducer of a nominal center frequency of 10 MHz (Panametrics V311) as the transmitting transducer. A 1 mm diameter PVDF, broadband, needle hydrophone (Force Institute) was used as the receiving transducer. The receiving hydrophone was scanned in a series of planes (32 sites by 32 sites with 0.5 mm separation between sites, 15.5 mm by 15.5 mm area total) at axial positions of 1", 2", and 3" from the transmitting transducer. These positions permitted measuring the ultrasonic field before the focal zone, within the focal zone, and after the focal zone of the transmitting transducer.

Figure 1 is a schematic diagram showing the data acquisition system used in this investigation. The ultrasonic signal sent to the transmitting transducer was a broadband pulse generated by a Metrotek MP215 pulser. The ultrasonic signal received by the hydrophone was initially sent through a unity-gain preamplifier (Force Institute) matched specifically to the hydrophone, providing 50 Ω coupling to the receive-side electronic equipment. The signal was then sent through a pair of step attenuators (HP 355 series) that permitted a more precise adjustment of the signal amplitude to prevent saturation of the input stage of the receiving electronic equipment. Further amplification was achieved by sending the received signal through a Metrotek MR106 rf

amplifier. The rf signal was digitized with a Tektronix 2430A digital oscilloscope. An Apple Macintosh II computer was used to read the rf time traces and store them for off-line analysis.

At each site of the pseudo-array, 64 time traces were acquired and averaged off-line before being stored to disk. Each rf time trace consisted of 1024 points sampled at 250 MegaSamples/s (0.004 μs sampling period). The digital oscilloscope was externally triggered by the synchronization pulse provided by the MP215 pulser. The data acquisition delay time (relative to the trigger signal) was set manually such that the received trace was localized within the acquisition window.

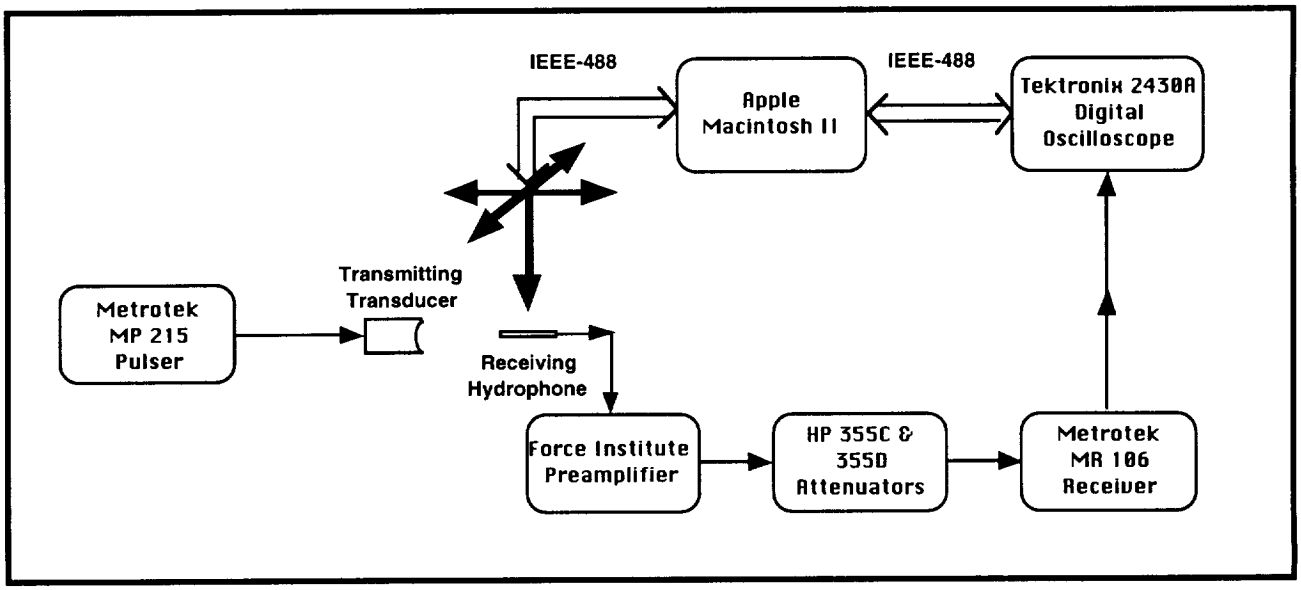

Figure 1: Experimental arrangement of data acquisition equipment

IV. Data Analysis / Modeling

Data analyses and computer modeling were performed using in-house custom software written in the C programming language on a Power Macintosh. These routines performed all the necessary tasks to calculate and visualize the simulated ultrasonic diffraction patterns, based on either the simulated or experimentally measured ultrasonic fields, using the method of Angular Spectral Decomposition. In order to construct images of continuous-wave ultrasonic fields, it was

necessary to calculate the in-phase and quadrature parts of the pressure field measured at each pseudo-array scan site. The averaged rf time trace acquired at each pseudo-array site was Fast Fourier Transformed. The real and imaginary parts of the Fourier transform corresponded to the in-phase and quadrature parts, respectively, of the received pressure field spectra. In order to use data from the broadband measurements in the continuous-wave based method of Angular Spectral Decomposition, single-frequency data was extracted from the in-phase and quadrature calculations providing narrow-band in-phase and quadrature representations of the field measured with the pseudo-array. These narrow-band representations were then imported into the in-house custom-designed software program to permit visualization of the propagated pressure fields.

Propagations from Experimentally Measured Field

For the experimental water path data, we imported the in-phase and quadrature parts of the experimentally measured pressure field at single frequencies (5.13 MHz, 7.08 MHz, and 11.2 MHz) at the receiver plane for each of the positions from the transmitting transducer (1", 2", and 3"). We zero-padded our 32 x 32 single-frequency in-phase and quadrature parts of the pressure field to 64 x 64 in order to minimize boundary effects (which can occur in the Fourier projection technique if array size is too small) as the fields were propagated. We applied a radial (from the center of the pseudo-array) Hanning window to the zero-padded in-phase and quadrature parts of the pressure field so as to prevent sharp discontinuities due to the padding. The measured ultrasonic pressure field was back-propagated to the transmitting transducer plane. Furthermore, the measured ultrasonic pressure field was forward-propagated to a distance of 4" from the transmitter transducer plane. (See Figure 2 on CD-ROM for an illustration of this procedure.) The distance between planes of propagation was 1 mm. The resulting diffraction patterns for the meridian plane views and the receiver plane views were constructed.

Propagations from Simulated Field

For visualizations of the simulated ultrasonic fields through water, we modeled our ultrasonic source as a 0.5" diameter, spherically-focused piston. Similar to our experimental data analysis, we used a 64 by 64 array with a 0.5 mm between sites. The distance between planes of propagation was 1 mm. We then propagated a single-frequency (5.13 MHz, 7.08 MHz, or 11.2 MHz) ultrasonic field for comparison to the experimental measurement. We simulated the ultrasonic pressure field that the hydrophone pseudo-array would see at distances of 1", 2", and 3" from the source plane. We also simulated the magnitude of the pressure fields in the meridian plane for a distance of up to 4" from the source plane.

Propagations from Experimentally Measured Field through Woven Composite Model

In order to build intuition of the diffraction effects due to anisotropic media, we simulated ultrasonic wave propagations through woven fiber composites. A woven fiber composite would diffract the ultrasonic field for several reasons, including: attenuation anisotropy, phase velocity anisotropy, and refraction at the woven layers due to non-normal incidence of ultrasound onto the warp and fill. As a first step in modeling an anisotropic material, our composite model consisted of a five-harness biaxial weave pattern, with the visible warp regions having 50% of the attenuation of the visible fill regions. The relative attenuations of the woven composite were chosen based on experimental measurements from previous work by this group[1]. An image of our composite model is shown in Figure 13 (see CD-ROM), with darker regions corresponding to the fill and the lighter regions corresponding to the warp of the weave pattern.

We imported the narrow-band (5.13 MHz) in-phase and quadrature parts of the pressure field measured by the hydrophone pseudo-array positioned 2" from the transmitting transducer. We again zero-padded our 32 x 32 narrow-band in-phase and quadrature parts of the pressure field to 64 x 64 in order to avoid boundary effects as the fields were propagated. Similarly, we applied a radial (from the center of the pseudo-array) Hanning window to the zero-padded in-phase and

quadrature parts of the pressure field so as to prevent sharp discontinuities due to the padding. To simulate the attenuation of a thin woven fiber composite coupon, we propagated the ultrasonic pressure field through the composite model, positioned at the focal plane of the transmitting transducer, to a distance 10 mm past the composite model. We generated images of the diffraction patterns for the receiver plane views of the magnitude, in-phase, and quadrature parts of the pressure field. The inclusion of the in-phase and quadrature images for the woven fiber composite investigation permits insight into the nature of phase cancellation across the face of the receiver transducer.

The experimental and simulated propagated fields were saved to disk and imported into a commercial imaging software package (Transform 3.3, Fortner Research LLC, Sterling, VA) for final production of the ultrasonic pressure field images. In the pressure magnitude images (receiver plane view image and meridian plane view two-dimensional image and surface plot), darker regions correspond to larger relative pressure magnitudes and lighter regions correspond to smaller relative pressure magnitudes. However, for the in-phase and quadrature parts of the pressure field, a blue to white to red color table has been used. Blue regions correspond to negative values, red regions correspond to positive values, and white regions are neutral. We chose to crop the receiver plane views of the ultrasonic in-phase, quadrature, and magnitude fields so that only the original 32 by 32 grid was shown. Cropping the images permitted zooming the region of interest and displaying the image on a scale exhibiting finer resolution.

V. Results

In this Section we discuss the images of the pressure magnitudes of the ultrasonic field in a meridian plane view and the receiver plane view, and images of the in-phase and quadrature parts of the pressure field in the receiver plane view. The images discussed here are for a single frequency (5.13 MHz) extracted from the broadband measurements. Two-dimensional images are shown of the magnitude of the pressure field at the receiver plane view for the water-path

simulations and experimental data. We also include two-dimensional images and surface plots of a meridian plane view of the water-path simulations and experimental measurements. For the woven fiber composite simulation, we include two-dimensional images of the magnitude, in-phase, and quadrature parts of the pressure field in the receiver plane view. Please see CD-ROM for all the images discussed in this Section.

The meridian plane views have dimensions of ~1.5 inches by 4.0 inches. (Please note the aspect ratio of 2.25:1.) The receiver plane views represent dimensions of ~0.75 inches by ~0.75 inches. In Figures 3 to 5 and Figures 7 to 12, the simulated images are constructed using the same uniformly-excited spherically-focused piston source parameters, and are provided in each figure for direct comparison to the different experimental situations.

Figure 3 compares the ultrasonic diffraction pattern in a meridian plane of the water-path only simulation and that obtained based on the field measurements of the receiving hydrophone 1" from the transmitting transducer. Figures 4 and 5 show similar images, with the position of the receiving hydrophone now at 2" and 3", respectively, from the transmitting transducer. Figure 2 shows the positioning of the transmitting transducer in relation to the propagated field in the meridian plane. In Figures 3 to 5 there are good qualitative agreement between simulation source and experimentally measured source in the depth and width of the focal zone. We also see agreement in the initial convergence of the source to the focal zone and the subsequent spreading of the ultrasonic field, as one would expect from a focused transducer.

Figures 7 to 9 are surface plots of the pressure magnitudes in the meridian plane. These figures present information about the pressure magnitude of the source across its face, in addition to the focal zone information of the ultrasonic field. Figure 6 shows a cartoon that identifies the position of the transmitting transducer relative to the surface plot of the ultrasonic field. In the upper left side of each surface plot, the transmitting transducer radiates downward to the right. In addition to the grayscale coding of the relative pressure magnitudes, the height of the surface plot corresponds to the relative pressure magnitude. (Please note the 2.67:1 aspect ratio in the plane normal to pressure magnitude.) We can make the same qualitative comments regarding the focal

zone as we did for Figures 3 to 5. In addition, the back-propagation of the experimentally received ultrasonic fields to the source plane shows the departure from our model of a uniformly excited piston source. We observe a gradual decline in pressure magnitude as we move to the edge of the transducer for the back-propagated experimentally measured fields. This raises the concern of the validity of modeling our source as being uniformly excited, or of the validity of the back-propagation model itself. We will address this further in Section VI.

Figures 10 to 12 compare the ultrasonic diffraction patterns in the receiver plane of the simulation and the water-path only experimental data at 1", 2", and 3", respectively. Again, we find good agreement between simulation and experimental measurement for the relative pressure magnitudes and the 3 dB-down regions (as noted by the red dashed circle) from the peak pressure.

Figure 13 shows an image of the attenuation mask of the woven fiber specimen model. As mentioned previously, the darker regions in the image correspond to regions of more attenuation, and the lighter regions corresponding to regions of less attenuation. Figures 14 to 22 contain images of the in-phase part, quadrature part, and magnitude of the pressure fields of the ultrasonic diffraction pattern in the receiver plane 10 mm beyond focal plane. Figures 14 to 17 compare the in-phase parts of the pressure fields of water-path only and through the composite model using different color tables and data ranges. By modifying the range of data imaged and adjusting the color table, we are able to emphasize different features of the images. Figures 14 and 15 use a linear color table. Figures 16 and 17, however, use a non-linear color table which emphasizes changes in the sign of the in-phase part of the pressure field. Similarly, Figures 18 to 21 compare the quadrature parts of the pressure fields of water-path only and through the composite model using different color tables and data ranges. We recognize a slight distortion of the in-phase and quadrature parts of the pressure field through the composite specimen model as compared to the in-phase and quadrature parts of the pressure field of the water-path only by comparing the shape of the central positive (red) region. However, in the images of the magnitude of the pressure field it is more difficult to discern changes between through water-path only and through the composite

model, as evidenced in Figure 22. (Please note similarity of 3 dB-down regions highlighted by the red dashed lines.)

VI. Discussion

We have implemented a systematic approach to enhance the understanding of the physics underlying the interaction of ultrasound with anisotropic materials. Initial investigations were performed to validate our technique of using an Angular Spectral Decomposition method to simulate experimental situations. In Figures 7 to 9, we compared the simulated source to the source predicted from back-propagation of the measured ultrasonic field. In future work, it may be advantageous to simulate a source with a smooth pressure variation out to the edge in contrast to a uniformly-excited piston source.

We extended our use of the Angular Spectral Decomposition method to model the possible effects that would occur in an anisotropic woven fiber composite. As a first step, we have considered only the magnitude attenuation effects, neglecting other pertinent effects, including phase velocity anisotropy and refraction at the surface that may occur. We observed in Figures 14 to 21 phase alterations, as compared to a water-path only signal, which could possibly produce phase cancellation across the face of the interrogating phase-sensitive transducer, thus underestimating the signal strength. Furthermore, knowledge of the diffraction effects of the anisotropy of the material will aid in linear, 1.5, and two-dimensional array beam forming.

These observations lead to several issues of concern for further investigation. In our model of a woven fiber composite, we have chosen a small tow size. It is worth investigating how adjusting tow size can affect the received signal. Furthermore, we have shown images constructed for 5.13 MHz. Increasing frequency will permit finer resolution of the constructed images. However, in the pursuit of a robust measurement technique, it is worth considering the issue of focal spot size versus spatial averaging.

References

1. T.D. Lhermitte, S.M. Handley, M.R. Holland, and J.G. Miller, "Anisotropy of the Frequency-Dependent Ultrasonic Attenuation in Unidirectional Graphite/Epoxy Composite Material", *Proc. IEEE Ultrasonics Symposium*, (Orlando, Published 1992), Vol. 91CH3079-1, pp. 819-823, (1991).

2. L. J. Busse, et al., "Phase Cancellation Effects: A Source of Attenuation Artifact Eliminated by a CdS Acoustoelectric Receiver", *Ultrasound in Medicine*, Vol. 3, pp. 1519-1535, (1977).

3. Patrick H. Johnston and J.G. Miller, "Phase-Insensitive Detection for Measurement of Backscattered Ultrasound", *IEEE Transactions on Ultrasonics, Ferroelectrics, and Frequency Control*, Vol. UFFC-33, pp. 713-721, (1986).

4. F. J. Margetan and R. B. Thompson, "The Use of Axial Pressure Field Scans to Characterize Spherically-Focussed Ultrasonic Transducers, and Results for Three Nominally Identical 5-MHz Probes", Center for Nondestructive Evaluation, Report Number: ISU/ETC-5, (June, 1994).

5. Mitchell M. Goodsitt, Ernest L. Madsen, and James A. Zagzebski, "Field patterns of pulsed, focused, ultrasonic radiators in attenuating and nonattenuating media", *J Acoust Soc Am*, Vol. 71, pp. 318-329, (1982).

6. Ernest L. Madsen, Mitchell M. Goodsitt, and James A. Zagzebski, "Continuous waves generated by focused radiators", *J Acoust Soc Am*, Vol. 70, pp. 1508-1517, (1981).

7. C. J. Bouwkamp, "Diffraction Theory", *Reports on Progress in Physics*, Vol. 17, pp. 35-92, (1954).

8. M. Forbes, S. Letcher, and P. Stepanishen, "A Wave Vector, Time-Domain Method of Forward Projecting Time-Dependent Pressure Fields", *J Acoust Soc Am*, Vol. 90, pp. 2782-2793, (1991).

9. Mark E. Schafer and Peter A. Lewin, "Transducer Characterization Using the Angular Spectrum Method", *J Acoust Soc Am*, Vol. 85, pp. 2202-2214, (1989).

10. Peter R. Stepanishen and Kim C. Benjamin, "Forward and Backward Projection of Acoustic Fields Using FFT Methods", *J Acoust Soc Am*, Vol. 71, pp. 803-812, (1982).

11. Christopher J. Vecchio and Peter A. Lewin, "Finite Amplitude Acoustic Propagation Modeling Using the Extended Angular Spectrum Method", *J Acoust Soc Am*, Vol. 95, pp. 2399-2408, (1994).

12. Robert C. Waag, James A. Campbell, Jan Ridder, and Peter R. Mesdag, "Cross-Sectional Measurements and Extrapolations of Ultrasonic Fields", *J Acoust Soc Am*, Vol. 32, pp. 26-35, (1985).